Top Catal (2010) 53:1039–1044
DOI 10.1007/s11244-010-9528-2

ORIGINAL PAPER

Hydrocarbon Oxidation with H_2O_2, Catalyzed by Iron Complexes with a Polydentate Pyridine-Based Ligand

Stefania Tanase · Jan Reedijk · Ronald Hage · Gadi Rothenberg

Published online: 2 June 2010

Abstract We report the structural and functional features of two new catalysts: a mononuclear $[Fe(N_5mpy)(CH_3CN)](BF_4)_2$ (N_5mpy = (*N*,*N*′E,*N*,*N*′E)-*N*,*N*′-(pyridine-2,6-diyl*bis*(ethan-1-yl-1-ylidene))*bis*(1-(pyridin-2-yl)methanamine)) complex and a binuclear $\{[Fe(N_5mpy)]_2O\}(BF_4)_4$ complex. Both compounds catalyze the oxidation of alkanes by H_2O_2, in MeCN or acetone to yield alcohols and ketones. Moderate to good yields are obtained with various cyclic and benzylic alkanes. Screening of several substrates revealed that higher yields are obtained for the oxidation of alkanes with low C–H bond dissociation energies. The ratio alcohol/ketone observed suggests the involvement of iron-based oxidizing species.

Keywords Iron · Pentadentate ligand · Catalytic oxidation

Electronic supplementary material The online version of this article (doi:10.1007/s11244-010-9528-2) contains supplementary material, which is available to authorized users.

S. Tanase (✉) · G. Rothenberg
Van't Hoff Insitute of Molecular Sciences, University of Amsterdam, Nieuwe Achtergracht 166, 1018 WV Amsterdam, The Netherlands
e-mail: s.grecea@uva.nl

S. Tanase · J. Reedijk
Gorlaeus Laboratories, Leiden Institute of Chemistry, Leiden University, PO Box 9502, 2300 RA Leiden, The Netherlands

R. Hage
Rahu Catalytics, BioPartner Center Leiden, Wassenaarseweg 72, 2333 AL Leiden, The Netherlands

1 Introduction

The selective catalytic oxidation of hydrocarbons is a key area of research in academia and industry [1–5]. While extreme reaction conditions (environmentally unfriendly oxidants, high temperature and/or pressure) are used in industry, nature has developed several strategies to selectively oxidize and functionalize hydrocarbons using metalloenzymes, such as iron bleomycin, methane monooxygenase, and Rieske oxygenase [6–8]. These enzymes can activate dioxygen and use it for oxidizing different substrates. Some of these iron-containing enzymes catalyze dihydrogen peroxide degradation (catalases), fatty acid oxidation or methane to methanol conversion. Thus, mimicking the action of such enzymes can result in new and eco-friendly catalytic processes [3, 5].

The most intensively studied complexes have tetradentate nitrogen-donor ligands with topologies that enable peroxide binding and activation to *cis*-oriented coordination sites [1, 2]. Others include iron(II) complexes containing pyridine-based pentadentate ligands, with two to five pyridine rings [9–16]. These complexes can react with H_2O_2, forming metastable Fe–OOH intermediates, and in some cases to catalyze alkane hydroxylation [11, 15]. However, many of these systems give only low conversion and low product selectivity. Formation of hydroxyl radicals using these $[FeN_5]$ complexes has been implicated, similarly to what has been described to Fenton-type chemistry. Earlier, one of us reported on an iron(II) complex containing the pentadentate ligand 6-*bis*[1-(2-methylanisolylimino)ethyl]pyridine (dapab) [17]. This complex completely converted cyclohexane to the corresponding ketone/alcohol mixture within 12 h. The low selectivity was explained by the involvement of hydroxyl radicals using this catalyst. Here we describe the structural and

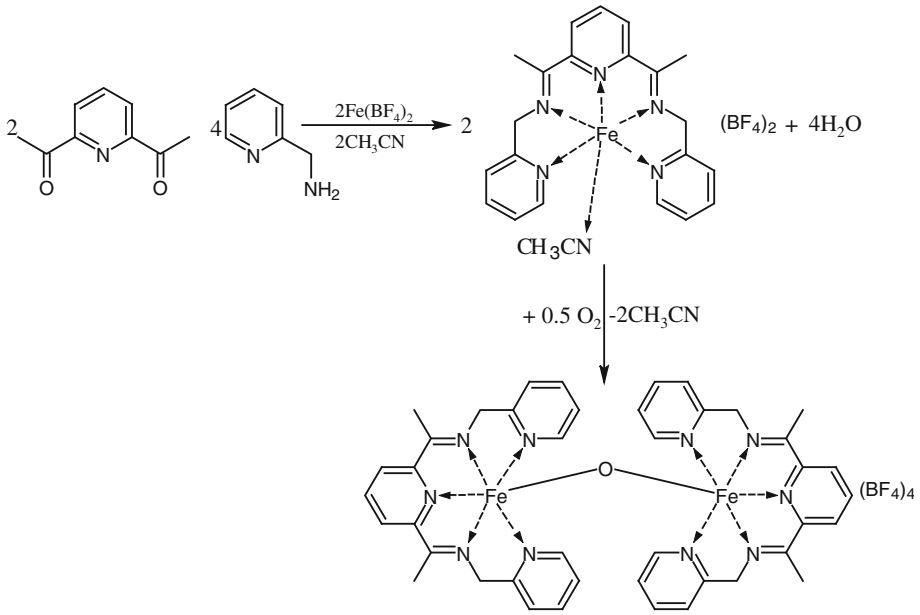

Fig. 1 Synthesis of the complexes $[Fe(N5mpy)(CH_3CN)](BF_4)_2$ **1** and $[Fe(N5mpy)(CH_3CN)](BF_4)_2$ **2**

functional features of two new iron(II) and (III) complexes containing a pentadentate pyridine-based ligand (N_5mpy = (*N*,*N*′E,*N*,*N*′E)-*N*,*N*′-(pyridine-2,6-diyl*bis*(ethan-1-yl-1-ylidene))*bis*(1-(pyridin-2-yl)methanamine)), namely the mononuclear $[Fe(N_5mpy)(CH_3CN)](BF_4)_2$ **1** and the binuclear $\{[Fe(N_5mpy)]_2O\}(BF_4)$ **2**, see Fig. 1. Two additional pyridine units in this new ligand have been introduced. These are essential for high catalytic activity and selectivity, reflecting the increased charge transfer from the metal to the ligand, and the stronger ligand field that stabilizes the intermediates responsible for metal-based oxidations.

2 Experimental Section

Starting materials were purchased from Merck or Aldrich and used as received unless noted otherwise. Spectroscopic grade solvents were used in syntheses and characterizations. Preparing and handling of air-sensitive complexes was carried out under nitrogen using standard Schlenk techniques.

2.1 Synthesis

2.1.1 $[Fe(N_5mpy)(CH_3CN)](BF_4)_2$ (1)

10 mmol of 2-(2-aminomethylpyridine) was added to a solution of 2,6-diacetylpyridine (5 mmol) in 50 mL of MeCN. The resulting yellow solution was stirred for 1 h, followed by the addition of 5 mmol of $Fe(BF_4)_2{\cdot}6H_2O$. The resulting purple solution was heated to reflux and stirred for 1 h and subsequently the solvent was removed under reduced pressure to yield a dark solid. The crude product was recrystallized twice from MeCN to give a purple crystalline precipitate. Yield: 70%. Anal.: calcd. for $C_{23}H_{24}N_6FeB_2F_8$: C 45.00, H 3.94, N 13.69; found: C 45.03, H 4.54, N 13.70. IR (ν_{max}/cm^{-1}): 3365 br, 1699 w, 1652 w, 1607 m, 1575 w, 1436 br, 1386 w, 1286 w, 1021 br, 808 m, 762 s, 668 m, 519 s. UV/Vis/NIR in MeCN, λ_{max}/nm: 264 ($\pi \rightarrow \pi^*$), 420 (MLCT), 590 ($^1A_1 \rightarrow {}^1T_1$). ESI-MS in MeCN: m/z = 340.2 (100%) $[Fe(N_5mpy)(CH_3CN)]^{2+}$.

2.1.2 $\{[Fe(N_5mpy)]_2O\}(BF_4)_4$ (2)

10 mmol of 2-(2-aminomethylpyridine) was added to a solution of 2,6-diacetylpyridine (5 mmol) in 50 mL of MeCN. The resulting yellow solution was stirred for 1 h, followed by the addition of 5 mmol of $Fe(BF_4)_2{\cdot}6H_2O$. The resulting purple solution was heated to reflux and stirred for 1 h and then the solvent was removed under reduced pressure to yield a dark solid. The resulted product was redissolved in MeCN and the resulting solution was kept in air for cause a color change from purple to green. Concentration of the green solution by slow evaporation of the solvent resulted in the formation of a green crystalline precipitate. Yield: 58%. Anal.: calcd. for $C_{42}H_{42}N_{10}OB_4F_{16}Fe_2$: C 43.42, H 3.73, N 12.05; found: C 42.66, H 3.51, N 12.58. IR (ν_{max}/cm^{-1}): 3382 br, 1694 s, 1600 m, 1570 m, 1431 m, 1342 s, 1297 s, 1236 m, 1061 br, 818 m, 762 s, 703 m, 646 w, 630 w, 593 m, 519 s. UV/Vis/NIR in MeCN, λ_{max}/nm: 267 ($\pi \rightarrow \pi^*$), 380 (LMCT), 495 (LMCT), 630 (LMCT).

2.2 Physical Methods

C, H and N analyses were performed with a Perkin-Elmer 2400 series II analyzer. Infrared spectra (4000–300 cm^{-1}, resolution 4 cm^{-1}) were recorded on a Perkin-Elmer Paragon 1000 FTIR spectrometer equipped with a Golden Gate ATR device, using the reflectance technique. The solution UV/Vis spectra of the compounds were recorded in the range of 200–1000 nm with a Cary 50 Varian UV/Vis/NIR spectrometer. The electrochemical measurements were performed with an Autolab PGstat10 potentiostat controlled by GPES4 software. A three-electrode system was used, consisting of a platinum working electrode, a platinum auxiliary electrode and an Ag/AgCl reference electrode. The experiments were carried at 25 °C under argon with tetrabutylammonium hexafluoridophosphate as the electrolyte. All potentials are reported relative to Ag/AgCl. ^{1}H NMR spectra were recorded on a DPX300 Bruker spectrometer using TMS as standard. GC-MS measurements have been obtained on Hewlett Packard 5890 Series II gas chromatograph equipped with a WCOT fused Silica column (stationary phase: CP-Was 58 (FFAP) CB) coupled to a Hewlett Packard 5971 series mass spectrometer with a mass selective detector.

Table 1 Product distribution for **1** (1 mM) catalyzed oxidation of different hydrocarbons in MeCN and acetone[a]

Substrate	Product	TON[e]		Yield (%)[f]	
		MeCN	Acetone	MeCN	Acetone
Cyclohexane	Cyclohexanol	3.6	2.3	44	29
	Cyclohexanone	0.8	0.6		
	A/K[b]	4.5	3.8		
Cyclooctane	Cyclooctanol	1.7	1.5	52	37
	Cyclooctanone	3.5	2.2		
	A/K[c]	0.5	0.7		
Adamantane	Adamantan-1-ol	3.5	2.8	58	45
	Adamantan-2-ol	1.6	1.2		
	Adamantan-2-one	0.7	0.5		
	C3/C2[d]	4.6	4.9		
Toluene	Benzaldehyde	5.1	4.5	62	52
	Benzylic alcohol	1.1	0.7		
	Benzoic acid	n.d.	n.d.		
Ethylbenzene	2-Phenyl-2-ethanol	3.8	3.2	64	51
	2-Phenyl-1-ethanol	1.4	1.1		
	Acetophenone	1.2	0.8		
Cumene	2-Phenyl-2-propanol	5.3	4.8	70	56
	2-Phenyl-1-propanol	n.d.	n.d.		
	Acetophenone	1.2	0.8		
	α-Methyl styrene	0.5	n.d.		

[a] Results after 1 h of reaction time and using a catalyst:substrate:H_2O_2 molar ratio of 1:1000:10, at 25 °C using MeCN as solvent. Results are given as mmol product/mmol catalyst

[b] Cyclohexanol to cyclohexanone ratio in the oxidation of cyclohexane

[c] Cyclooctanol to cycloctanone ratio in the oxidation of cyclooctanone

[d] C3/C2 = 3 × adamantan-1-ol/(adamantan-2-ol + adamantan-2-one) in the oxidation of adamantane

[e] Mol of product per mol of catalyst

[f] Conversion based on H_2O_2

Table 2 Product distribution for **2** (1 mM) catalyzed oxidation of different hydrocarbons in MeCN and acetone[a]

Substrate	Product	TON[e]		Yield (%)[f]	
		MeCN	Acetone	MeCN	Acetone
Cyclohexane	Cyclohexanol	3.6	2.8	41	30
	Cyclohexanone	0.5	0.2		
	A/K[b]	7.2	1.4		
Cyclooctane	Cyclooctanol	2.1	0.8	57	20
	Cyclooctanone	3.6	1.2		
	A/K[c]	0.6	0.7		
Adamantane	Adamantan-1-ol	2.2	0.9	29	10
	Adamantan-2-ol	0.5	0.2		
	Adamantan-2-one	0.2	n.d		
	C3/C2[d]	9.4	13.5		
Toluene	Benzaldehyde	n.d	n.d.	11	9
	Benzylic alcohol	1.1	0.9		
	Benzoic acid	n.d.	n.d.		
Ethylbenzene	2-Phenyl-2-ethanol	2.8	2.4	44	32
	2-Phenyl-1-ethanol	0.4	n.d		
	Acetophenone	1.2	0.8		
Cumene	2-Phenyl-2-propanol	4.3	3.8	61	38
	2-Phenyl-1-propanol	n.d.	n.d.		
	Acetophenone	1.3	n.d.		
	α-Methyl styrene	0.5	n.d.		

[a] Results after 1 h of reaction time and using a catalyst:substrate:H_2O_2 molar ratio of 1:1000:10, at 25 °C using MeCN as solvent. Results are given as mmol product/mmol catalyst

[b] Cyclohexanol to cyclohexanone ratio in the oxidation of cyclohexane

[c] Cyclooctanol to cycloctanone ratio in the oxidation of cyclooctanone

[d] C3/C2 = 3 × adamantan-1-ol/(adamantan-2-ol + adamantan-2-one) in the oxidation of adamantane

[e] Mol product per mol catalyst

[f] Conversion based on H_2O_2

2.3 Catalytic Experiments

In a typical run, 50 μmol of H_2O_2 (30%) were added to an MeCN solution (5 mL) containing 5 μmol catalyst and 5 mmol alkane (cyclohexane, cyclooctane or adamantane) at 25 °C. The catalyst:substrate:H_2O_2 ratio was 1:1000:10. Periodically, aliquots were taken from the reaction mixtures and analyzed twice by GC-MS: with and without adding an excess of triphenylphosphane for quantifying the hydroperoxide. All products formed were identified by GC and retention times compared with commercially available products. Product yields were calculated as shown in Tables 1 and 2 (based on GC area corrected by the presence of chlorobenzene as internal standard) and the sum of oxidation products formed match the fraction of the substrate converted.

3 Results and Discussion

The template condensation of 2,6-diacetylpyridine with 2-(2-aminomethylpyridine) in the presence of $Fe(BF_4)_2 \cdot 6H_2O$ affords complex **1** in 70% yield. Microanalytical and spectroscopic data suggest that **1** has the formula $[Fe(N_5mpy)(CH_3CN)](BF_4)_2$. The IR spectrum of **1** clearly indicates the presence of BF_4^- ions (1021 and 668 cm^{-1}) as well as the presence of the N_5mpy ligand; the strong and narrow band at 762 cm^{-1} is characteristic of the aromatic skeleton vibration while the bands at 1607 and 1436 cm^{-1} are due to the stretching vibrations ν_{C-N} and $\nu_{C=N}$, respectively [18]. The solid-state ligand field spectrum displays a MLCT transition band at 420 nm and another band at 590 nm, assigned to the $^1A_1 \rightarrow {}^1T_1$ transition of the low-spin iron(II) [19]. In MeCN, besides the bands at 370 nm (MLCT, $\varepsilon = 2820\ M^{-1}\ cm^{-1}$) and 570 nm ($^1A_1 \rightarrow {}^1T_1$, $\varepsilon = 2370\ M^{-1}\ cm^{-1}$) due to the low-spin species, a shoulder at 490 nm indicates that some contribution of the high-spin iron(II) state may also be present in solution (see supporting information for details) [19]. These results agree with the cyclic voltammetry studies, that show two anodic reversible waves at $E_{1/2} = 0.47$ V and $E_{1/2} = 0.68$ V versus Ag/AgCl, assigned to two-one-electron transformation Fe(II) → Fe(III). The relatively low values reflect the thermodynamic instability of the iron(II) complex in air. The mononuclear structure of **1** in MeCN was shown by the positive-ion electrospray MS data obtained at 1 mM concentration (m/z = 340.2 $[Fe(N_5mpy)(CH_3CN)]^{2+}$).

Compound **1**, however, is air- and water-sensitive, both as a solid and in solution. Its stability in solution is limited to few hours under nitrogen, and it is unstable in the presence of oxygen. The initial purple color turns to green in less than an hour in air, yielding complex **2**. Therefore, **2** was prepared by the aerobic oxidation of **1** (see Fig. 1). The IR spectrum of **2** shows the characteristic bands of the ligand (vide infra) and of BF_4^- (1016 and 630 cm^{-1}). The ν_{asymm} and ν_{symm} stretching vibrations for the Fe–O–Fe core are suspected to be responsible of the bands at 818 and 593 cm^{-1}, respectively [20]. The ligand field spectrum of **2** in the solid state shows the main bands due to the Fe–O–Fe core: at 370 nm, a LMCT band independent of the Fe–O–Fe; at 495 nm due to a $^6A_1 \rightarrow ({}^4E,{}^4A_1)$ transition, the intensity of which is enhanced by a partial overlapping with the LMCT band; and at 630 nm due to a $^6A_1 \rightarrow {}^4T_2$ transition, suggesting a bent Fe–O–Fe angle [21]. The ligand field spectrum of **2** in MeCN shows the same characteristics, but all bands are slightly blue-shifted. The ^1H NMR of **2** in CD_3CN shows broad signals in the 0–15 ppm range (Fig. 2). This suggests that the dinuclear μ-oxidodiiron(III) core remains stable in solution, reflecting the presence of strong antiferromagnetic interactions between the two iron(III) ions as also suggested by the temperature magnetic susceptibility data (see supporting information) [22]. The cyclic voltammogram of compound **2** recorded at 25 °C in MeCN shows two irreversible one-electron reduction waves at $E_{1/2} = -0.45$ V and $E_{1/2} = -0.66$ V versus Ag/AgCl, corresponding to the Fe(III) → Fe(II) reduction of the metal centers (Fig. 3). After a first redox cycle, an anodic peak appears at $E_{1/2} = 0.49$ V versus Ag/AgCl, the intensity of which increases and reaches a steady-state after five scans. This indicates that upon reduction the dinuclear unit rearranges to mononuclear species.

Due to the air sensitivity of **1**, all characterizations and manipulation for catalytic studies were performed under argon. Unfortunately, several attempts to obtain X-ray grade crystals of **1** and **2** failed. Proposed structures for compounds **1** and **2** are schematically depicted in Fig. 1.

The catalytic activities of **1** and **2** were tested in the oxidation of cyclohexane, cyclooctane, adamantane, toluene, ethylbenzene and cumene in MeCN and acetone at ambient conditions and over a 180 min period. The reaction was quenched after 1 h as control experiments showed

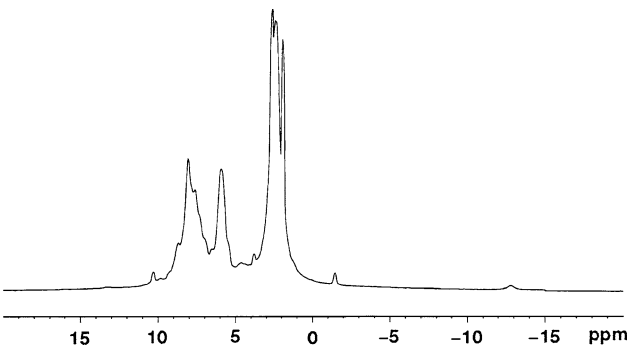

Fig. 2 ^1H NMR spectrum of **2** in MeCN solution at 25 °C

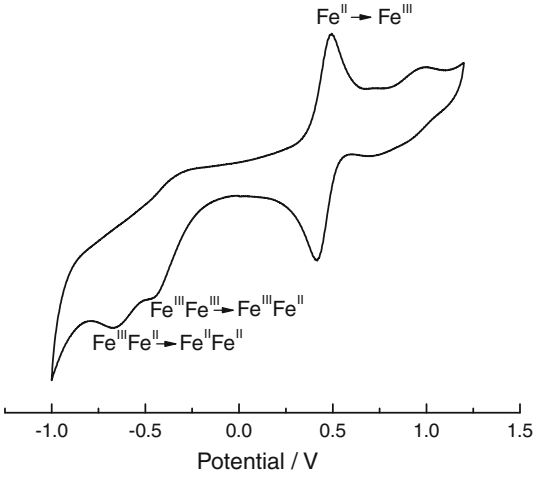

Fig. 3 Cyclic voltammogram of **2** in MeCN at 25 °C

no significant differences between 1 and 3 h. Tables 1 and 2 give the product distributions.

Using catalyst **1**, when the reaction is performed in MeCN and the substrate used is cyclohexane, the main product is cyclohexanol (A), while cyclohexanone (K) is the minor product (A/K = 4.5). Thus, a conversion of 44% based on oxidant was achieved. The conversion dropped to 29% when the reaction was carried out in acetone (A/K = 3.8), a known scavenger of oxygen-centered radicals. Using MeCN as solvent but with a higher H_2O_2 amount (50 or 100 equiv.), a lower conversion based on oxidant (up to 20%) as well as of a decrease of the A/K ratio (A/K = 1.1) was observed for the oxidation of cyclohexane. This difference is most likely due to an increase in nonproductive processes such as H_2O_2 decomposition and over-oxidation of cyclohexanol to cyclohexanone. Indeed, the A/K ratio decreases with time when large amounts of H_2O_2 are used, thus indicating that the over-oxidation of the alcohol to ketone does occur. The oxidation of cyclooctane was more efficient, with a final conversion based on oxidant of 52 and 29% in MeCN and acetone, respectively. Here, the ketone was found as the main product, with A/K ratios of 0.5 and 0.7, respectively [23, 24]. The regioselectivity studied by means of the C3/C2 ratio in adamantane oxidation, shows a slight enhancement when the reaction is performed in acetone with respect to MeCN (C3/C2 = 4.6 in MeCN and C3/C2 = 4.9 in acetone). Thus, same oxidizing species in MeCN and acetone might be involved. The non-selective HO• typically affords a C3/C2 ratio of ca. 2, whereas more selective oxidants give substantially higher values. For example, values of 3.1–3.3 for $[Fe(N4py)(CH_3CN)](ClO_4)_2$ were observed [15]. The relatively low C3/C2 ratio observed for catalyst **1** implies that the present catalytic reactions are distinct from a Fenton type free-radical oxidation reaction for which the typical C3/C2 ratios are higher than 20 [25]. In both MeCN and acetone, catalyst **1** oxidizes the substrates ethylbenzene and cumene with weak C–H bonds. The catalytic oxidation of ethylbenzene yielded both alcohols and ketone with a total conversion based on oxidant of 64 and 51%, respectively. Acetophenone was found as the minor product (A/K = 3.5 in MeCN and 4.1 in acetone). The oxidation of cumene proceeds with a conversion based on oxidant of 70% in MeCN (A/K = 4.4) and 56% in acetone (A/K = 6). The oxidation of ethylbenzene and cumene to alcohols and acetophenone clearly suggest the capture of an alkyl radical by a reactive Fe(III)–OOH intermediate, similar to the oxygen rebound step proposed for the heme-catalyzed hydroxylation, or the electron transfer between the alkyl radical and the iron(III)-alkylperoxo intermediate [3].

Catalyst **2** was less efficient in alkane hydroxylation compared with **1**. The results in Table 2 show that for compound 2, the higher activities were also obtained for the oxidation of alkanes with low C–H bond dissociation energies, such as ethylbenzene and cumene. Noteworthy, there is significant reduced efficiency for the oxidation of toluene by catalysts **2** as compared with catalyst **1**. These observations agree with our previous work [23, 24] on the oxidation of alkanes catalyzed by a μ-oxidodiiron(III) complex, as well as with the results reported for the oxidation of similar substrates by $[Fe(N4py)(CH_3CN)](ClO_4)_2$ in the presence of PhIO as oxidant [26]. Using MeCN, the A/K ratio of 7.2 in cyclohexane oxidation as well as the significant C3/C2 ratio of 9.4 observed for the oxidation of adamantane indicates the involvement of a metal-based oxidant.

4 Conclusions

We have synthesized and characterized two new iron complexes containing a pyridine-based pentadentate ligand and studied their ability to carry out alkane hydroxylation using dihydrogen peroxide as oxidant. The complexes show the spectral and electrochemical properties corresponding to a mononuclear Fe(II) low-spin compound and a μ-oxidodiiron(III) compound, respectively. The observation of high selectivity towards alkane hydroxylation points to the involvement of an intermediate metal-based oxidant rather than a free-radical oxidant. The very low TON are obtained partly because of small amounts of H_2O_2 used. Nevertheless, an increasing TON can be obtained by slow addition of H_2O_2 used. A significant challenge remains putting these results into practice in ways that are used for industrial and fine-chemical synthesis.

Acknowledgments We thank Daniele Cappellini for the synthesis of the compounds, Dr. Elisabeth Bouwman (UL) for valuable discussions and the Dutch Economy, Ecology, Technology (EET)

program (a joint program of the Ministry of Economic Affairs, the Ministry of Education, Culture and Science, and the Ministry of Housing, Spatial Planning and the Environment) for contributions to the funding.

References

1. Que L, Tolman WB (2008) Nature 455:333
2. Tanase S, Bouwman E (2006) Adv Inorg Chem 58:29
3. Meunier B (2000) Biomimetic oxidations catalyzed by transition metal complexes. Imperial College Press, London
4. Rothenberg G (2008) Catalysis: concepts and green applications. Wiley-VCH, Weinheim
5. Tolman WB (2006) Activation of small molecules: organometallic and bioinorganic perspectives. Wiley-VCH, Weinheim
6. Costas M, Mehn MP, Jensen MP, Que L (2004) Chem Rev 104:939
7. Solomon EI, Brunold TC, Davis MI, Kemsley JN, Lee SK, Lehnert N, Neese F, Skulan AJ, Yang YS, Zhou J (2000) Chem Rev 100:235
8. Tshuva EY, Lippard SJ (2004) Chem Rev 104:987
9. Balland V, Banse F, Anxolabehere-Mallart E, Ghiladi M, Mattioli TA, Philouze C, Blondin G, Girerd JJ (2003) Inorg Chem 42:2470
10. Balland V, Banse F, Anxolabehere-Mallart E, Nierlich M, Girerd JJ (2003) Eur J Inorg Chem 13:2529
11. Balland V, Mathieu D, Pons-Y-Moll N, Bartoli JF, Banse F, Battioni P, Girerd JJ, Mansuy D (2004) J Mol Catal A 215:81
12. Goldsmith CR, Jonas RT, Stack TDP (2002) J Am Chem Soc 124:83
13. Jensen KB, McKenzie CJ, Nielsen LP, Pedersen JZ, Svendsen HM (1999) Chem Commun 1313
14. Roelfes G, Lubben M, Chen K, Ho RYN, Meetsma A, Genseberger S, Hermant RM, Hage R, Mandal SK, Young VG, Zang Y, Kooijman H, Spek AL, Que L, Feringa BL (1999) Inorg Chem 38:1929
15. Roelfes G, Lubben M, Hage R, Que L, Feringa BL (2000) Chem Eur J 6:2152
16. Taktak S, Ye WH, Herrera AM, Rybak-Akimova EV (2007) Inorg Chem 46:2929
17. Tang JK, Gamez P, Reedijk J (2007) Dalton Trans 4644
18. Nakamoto K (1963) Infrared spectra of inorganic and coordination compounds. Wiley, New York
19. Hauser A, Vef A, Adler P (1991) J Chem Phys 95:8710
20. Solomon eI, Brunold TC, Kemsley JN, Lee SK, Lehnert N, Neese F, Skulan AJ, Yang Ys (2000) J Zhou Chem Rev 100:235
21. Norman RE, Holz RC, Menage S, Oconnor CJ, Zhang JH, Que L (1990) Inorg Chem 29:4629
22. Gorun SM, Lippard SJ (1991) Inorg Chem 30:1625
23. Tanase S, Foltz C, de Gelder R, Hage R, Bouwman E, Reedijk J (2005) J Mol Catal A 225:161
24. Tanase S, Marques-Gallego P, Browne WR, Hage R, Bouwman E, Feringa BL, Reedijk J (2008) Dalton Trans 2026
25. Appleton AJ, Evans S, Smith JRL (1996) J Chem Soc Perkin Trans 3:281
26. Kaizer J, Klinker EJ, Oh NY, Rohde JU, Song WJ, Stubna A, Kim J, Munck E, Nam W, Que L (2004) J Am Chem Soc 126:472